Nanoscale Advances

ROYAL SOCIETY OF CHEMISTRY

PAPER

View Article Online
View Journal | View Issue

Cite this: *Nanoscale Adv.*, 2024, **6**, 3911

Functionalized graphene oxide by 4-amino-3-hydroxy-1-naphthalenesulfonic acid as a heterogeneous nanocatalyst for the one-pot synthesis of tetraketone and tetrahydrobenzo[*b*]pyran derivatives under green conditions†

Sara Gharghish, Mohammad G. Dekamin * and Sepideh Hasanzadeh Banakar

4-Amino-3-hydroxy-1-naphthalenesulfonic acid-functionalized graphene oxide (GO-ANSA) was prepared and characterized using different spectroscopic, microscopic and analytical methods including energy-dispersive X-ray spectroscopy (EDS), EDS elemental mapping, Fourier-transform infrared (FT-IR) spectroscopy, field emission scanning electron microscopy (FESEM), X-ray diffraction (XRD), and thermogravimetry/differential thermogravimetry analysis (TGA/DTA). The obtained nanomaterial was used as a novel, highly efficient, and reusable solid acid carbocatalyst for the one-pot three-component synthesis of tetraketone, as well as tetrahydrobenzo[*b*]pyran derivatives *via* tandem Knoevenagel–Michael reactions under green conditions. All of the derivatives were prepared in EtOH, as a green solvent, under reflux conditions in high to excellent yields and very short reaction times. The nanocatalyst was recovered and reused at least five times without significant reduction in its activity. In addition, the absence of toxic transition metals, high to excellent yields, mild reaction conditions, simple procedure for the separation and purification of products, stability, and recycling of the catalyst are the most important advantages of this green procedure.

Received 17th March 2024
Accepted 23rd May 2024

DOI: 10.1039/d4na00223g

rsc.li/nanoscale-advances

1. Introduction

Most recently, nanotechnology has found extensive application across many fields and become one of the attractive topics among different fields of science and technology, including chemistry, physics, biology, materials, medicinal, electronic,[1] automotive,[2] aerospace,[3] and others.[4–6] One of the most important applications of nanotechnology in the field of chemistry is the preparation of nanocatalysts, which have shown a significant impact on green chemistry.[7–13] Indeed, a variety of inorganic and organic compounds have been reported as homogeneous catalytic species; however, they have disadvantages such as difficult separation and recycling, producing large quantities of hazardous waste, high cost, *etc.* To address these concerns, heterogeneous catalytic systems were introduced as alternatives for the homogeneous catalytic systems. In recent decades, nanocatalytic systems have emerged as a bridge between homogeneous and heterogeneous catalytic systems and demonstrate many advantages such as high activity, stability, and selectivity compared to the traditional catalytic systems. Among the catalyst supports, carbon materials are noteworthy due to their synergistic catalytic activation.[14–19]

Due to their unique properties, carbon-based nanomaterials have strongly influenced many research fields such as pollutant adsorption,[20] drug delivery,[21] biomedical imaging,[22] sensing,[23] and catalysis.[24] Graphene oxide (GO) is attracting special attention in many research fields such as antimicrobial nanohybrids,[25] batteries,[26] nanomembranes,[27] photocatalytic degradation of organic pollutants,[28] and supported catalysts[29,30] owing to its unique and exclusive properties including excellent chemical stability, high specific surface area, outstanding mechanical performance, and high thermal stability.[31–33] Because of its oxygen-containing functional groups such as hydroxyl, epoxide, and carboxylic acid on both surface and edges, GO has resolved the non-dispersion of graphene sheets in aqueous media. Consequently, it has more active sites for the loading of catalytically active species than pristine graphene. These properties make GO an attractive candidate for a catalytic substrate in synthesizing organic materials, especially *via* MCRs.[34–40]

MCRs are synthetic processes that simultaneously afford products from several reactants in one-pot reactions. Recently, a wide range of MCRs have been developed using various catalysts.[41–47] MCR procedures have many advantages such as reducing product purification processes, good atom economy, preventing the formation of side products, reducing the use of

Pharmaceutical and Heterocyclic Compounds Research Laboratory, Department of Chemistry, Iran University of Science and Technology, Tehran 16846-13114, Iran. E-mail: mdekamin@iust.ac.ir

† Electronic supplementary information (ESI) available. See DOI: https://doi.org/10.1039/d4na00223g

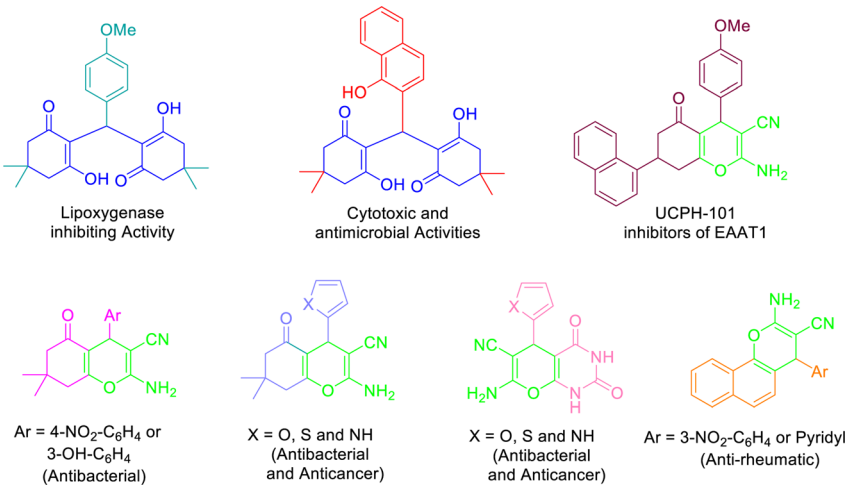

Fig. 1 Structure of selected examples of biologically- and pharmacologically-active tetraketones and 4*H*-pyrans.

solvents, and mild reaction conditions. MCRs are very attractive processes for the synthesis of a variety of polymers, heterocyclic compounds, and materials with biological properties, and provide a wide range of products often having complex molecular structures in rapid and simple procedures.[48–51] One of the most important parameters in the synthesis of organic compounds through MCRs and complying with the principles of green chemistry is choosing an eco-friendly solvent. In this context, performing the reactions for the synthesis of pharmaceutical intermediates or final active pharmaceutical ingredients (APIs) in EtOH, as a green solvent, is one of the best strategies.[9,41,52,53]

Recently, tetraketone and tetrahydrobenzo[*b*]pyran derivatives have attracted much attention due to their biological and medicinal properties. Tetraketones are a group of chemical compounds that exist in two forms (enol–keto tautomerism) and have antiviral,[54] antibacterial, antioxidant[55] as well as inhibitory properties of some enzymes such as lipoxygenase[56] or tyrosinase (reduce overproducing skin melanoma).[57] Also, these compounds are used in fabrication of laser dyes[58] and considered the most popular precursors for the preparation of many important organic compounds such as acridindiones and xanthendiones.[59]

On the other hand, tetrahydrobenzo[*b*]pyrans are non-aromatic heterocyclic compounds that were first synthesized in 1962 through the thermal decomposition of 2-acetoxy-3,4-dihydro-2*H*-pyran. These compounds have many biological properties including antioxidant, antitumor or anticancer, antianaphylactic, antispasmodic, and antiinflammatory.[35,60–63] Also, recent studies have shown that these heterocycles can be effective in the treatment of some diseases such as Alzheimer's, Down's syndrome, Schizophrenia, Parkinson's, *etc.* (Fig. 1).[49,64,65]

Different protocols have been introduced for the synthesis of tetraketone and tetrahydrobenzo[*b*]pyran derivatives by using a variety of catalysts in recent years.[66,67] So far, numerous heterogeneous and homogeneous catalysts for the synthesis of tetraketones such as [H-Pyrr][HSO_4],[68] L-histidine in ionic liquid,[69] nano SiO_2Cl,[70] amino-appended β-cyclodextrin,[71] $Cu_2(NH_2\text{-BDC})_2(DABCO)$,[72] Fe-zeolite,[73] and 2-aminopyrazine[74] have been reported. Similarly, a wide range of methods have been developed for the synthesis of tetrahydrobenzo[*b*]pyrans using different catalytic systems such as sodium alginate,[75] piperazine–GO,[76] SO_3H-functionalized nano-MGO-D-NH_2,[77] Cs-EDTA-Cell network,[78] nano α-Al_2O_3 supported ammonium dihydrogen phosphate ($NH_4H_2PO_4/Al_2O_3$),[79] proline- or

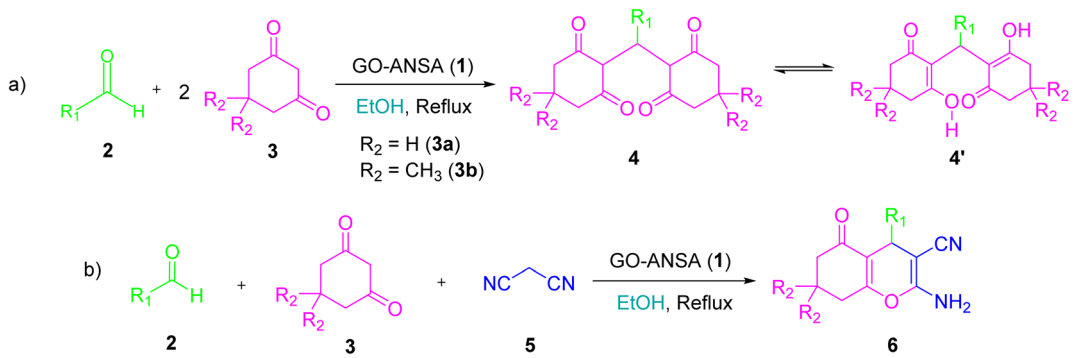

Scheme 1 One-pot three-component reaction of (a) aldehydes and enolizable compounds (2.0 equiv.), (b) aldehydes, enolizable compounds, and malononitrile catalyzed by the GO-ANSA nanomaterial.

propylamine-modified SBA-15,[80] PMO-ICS,[81] and $FeNi_3$–SiO_2 nanoparticles.[82] To the best of our knowledge, there are no previous reports on the use of GO-ANSA for the synthesis of organic compounds. In continuation of our interest for exploring various solid acid nanocatalysts in different organic transformations, especially based on GO,[83–88] we wish herein to report the catalytic activity of GO-ANSA (**1**) in the one-pot three-component reaction of aldehydes, enolizable compounds and/or malononitrile to afford the corresponding tetraketones or tetrahydrobenzo[*b*]pyrans (Scheme 1).

2. Experimental

2.1 Materials and measurements

$NaNO_3$ (98+%) was purchased from Sigma-Aldrich. Graphite flakes (99.8%), H_2SO_4 (98%), potassium permanganate ($KMnO_4$, 98.5%), HCl (37%), H_2O_2 (30%), acetic anhydride, 4-amino-3-hydroxy-1-naphthalenesulfonic acid (96%), dimedone, 1,3-cyclohexanedione, benzaldehyde derivatives, malononitrile, DMF and EtOH (96%) were purchased from Merck. Distilled water was used in all required steps of reactions or purification. The XRD pattern was collected by a D8 advance Bruker with Cu K_a radiation (λ = 1.54050 Å). FESEM images, EDX and EDX mapping were taken by FESEM TESCAN-MIRA3. Atomic force microscopy (AFM, Full PLUS, Brisk, ARA Research) was used to visualize the surface morphology of the sample. FTIR spectroscopy was performed on a 1720-X PerkinElmer. TGA-DTA analysis was performed by SPA-503 BAHR. ^{1}H NMR spectroscopy was carried out on a Bruker DRX-500 at 500 MHz using $CDCl_3$ and DMSO, as solvent, and data are given in ppm relative to TMS at ambient temperature ($CDCl_3$: ^{1}H: δ = 7.26 ppm). All the products are known compounds and were identified by comparison of their physical, spectroscopic, and analytical data with the authentic samples.

2.2 Synthesis of GO

GO was prepared *via* the modified Hummers' method.[89] The mixture of graphite (1.0 g) and $NaNO_3$ (0.5 g) was added to the concentrated sulfuric acid solution (23.0 ml, 98%), and stirred while the reaction temperature was kept below 4 °C. Then, $KMnO_4$ (3.0 g) was added at 20 °C and the stirring of the mixture was continued for 2 h until the reaction was complete. To avoid a sudden increase in the reaction temperature due to the exothermic nature of the reaction, $KMnO_4$ was slowly added to the mixture. After that, distilled water (46.0 ml) was slowly added to the reaction mixture at a temperature of 96 °C. In the next step, distilled water (140.0 ml) was added and finally, hydrogen peroxide (10.0 ml, 30% v/v) was added until the color of the mixture turned to yellow. Then, the obtained mixture was allowed to rest for 24 h, and it was washed with HCl (5%) solution and distilled water, so that all the impurities were washed and removed. Finally, the obtained GO was dried in an oven at 60 °C.

2.3 Synthesis of 4-amino-3-hydroxy-1-naphthalenesulfonic acid-functionalized graphene oxide (GO-ANSA, 1)

DMF (20.0 ml) and GO (200.0 mg) were added to a round-bottom flask and dispersed with an ultrasonic probe to separate the GO sheets. Afterward, Ac_2O (0.4 ml) was added to the sonicated solution and the obtained mixture was placed in an ultrasonic bath for 2.0 h. Then, ANSA (0.4 g) and Et_3N (0.35 ml) were added, and the mixture was stirred at 80 °C for 48 h. At the end of the reaction, sulfuric acid (0.1 ml) was added to the mixture. Then, the obtained residue was filtered using filter paper, and washed with THF and EtOH. Finally, the obtained black powder was dried at ambient temperature for 4 h (Scheme 2).

2.4 General procedure for the synthesis of tetraketone 4 and tetrahydrobenzo[*b*]pyran 6 derivatives catalysed by the GO-ANSA nanocatalyst

For the synthesis of the tetraketone derivatives **4**, aldehyde derivative (**2**, 1.0 mmol), enolizable compound (**3**, 2.0 mmol), GO-ANSA (**1**, 15.0 mg), as a nanocatalyst, and EtOH (3.0 ml) were added to a 10 ml flask under stirring and reflux conditions. The progress of the reaction was followed by TLC (*n*-hexane : EtOAc,

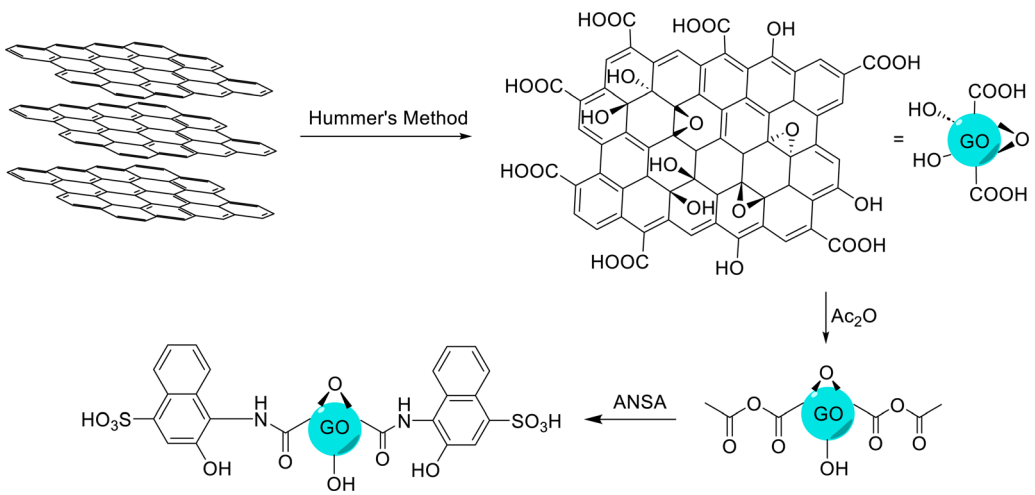

Scheme 2 Procedures for the preparation of GO, according to the modified Hummers' method, and subsequent preparation of GO-ANSA.

1 : 3). After the completion of reaction, EtOH (2 ml) was added to the mixture and it was heated to remove the catalyst from crude reaction mixture by filtration. Then, the pure products **4** were recrystallized from the ethanolic filtrate. The products were identified by measurement of their melting point as well as FTIR and ^{1}H NMR spectral data. The results are reported in Table 2.

For the synthesis of the tetrahydrobenzo[*b*]pyran derivatives **6**, the aldehyde derivative (**2**, 1.0 mmol), malononitrile (**5**, 1.0 mmol), enolizable compound (**3**, 1.0 mmol), GO-ANSA (**1**, 10.0 mg) and EtOH (3.0 ml) were added to a 10 ml round-bottom flask equipped with a magnetic stirring and reflux condenser. The progress of the reaction was monitored by TLC (*n*-hexane : EtOAc, 1 : 3). After the completion of reaction, EtOH (2 ml) was added to the mixture and it was heated to remove the catalyst from crude reaction mixture by filteration. Then, the pure products **6** were recrystallized from the ethanolic filtrate. The products were identified by measurement of their melting point

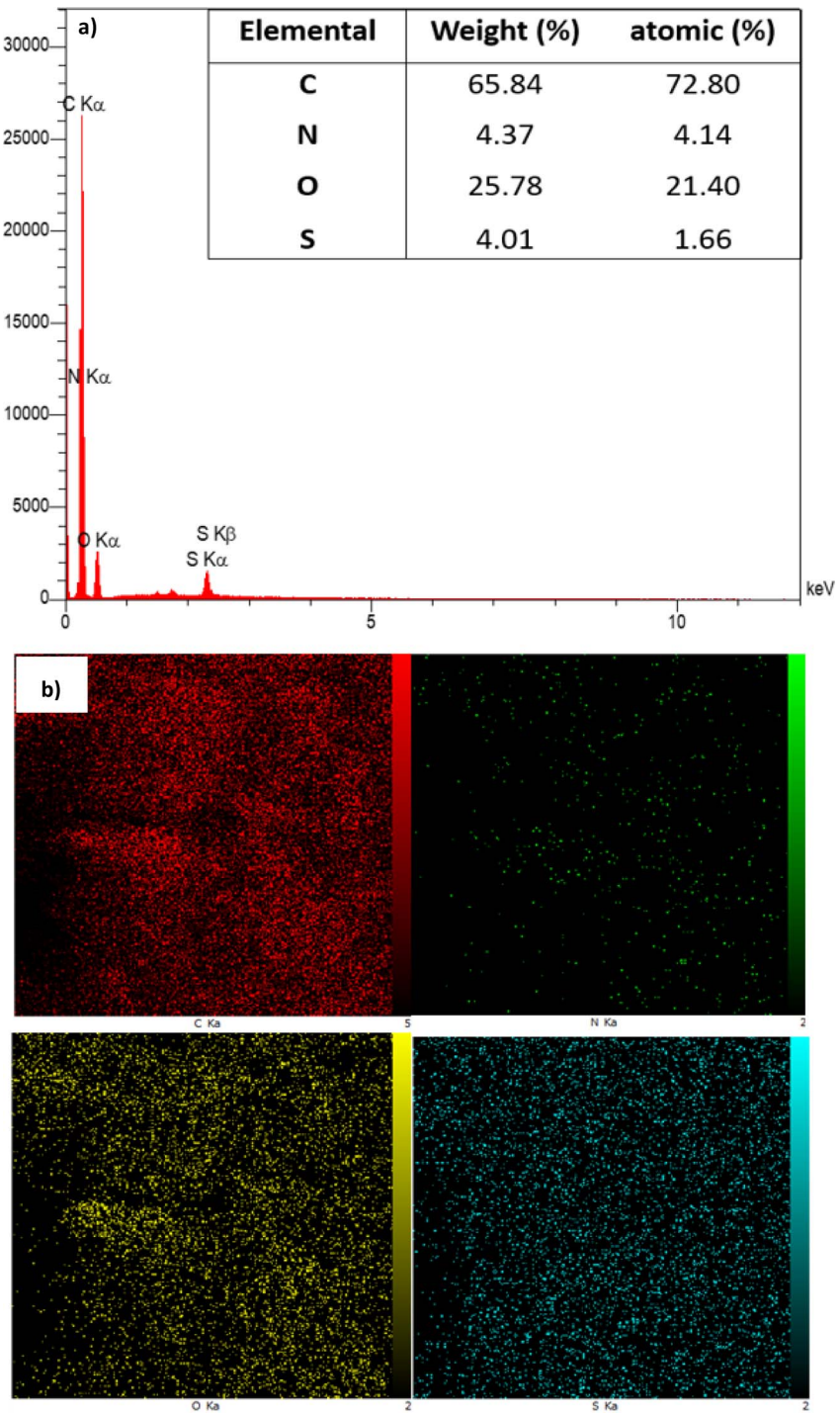

Fig. 2 (a) EDS spectrum and (b) EDS elemental mapping of GO-ANSA (**1**) for the distribution of C, N, O, and S atoms, respectively.

as well as FTIR and ^{1}H NMR spectral data. The results are reported in Table 5.

3. Results and discussion

3.1 Characterization of GO and GO-ANSA

To determine the percentage of different atoms present in the structure of GO-ANSA (**1**), both energy-dispersive X-ray spectroscopy (EDS, Fig. 2a) and EDS elemental mapping were used (Fig. 2b). According to the data for the EDX spectra of the GO-ANSA, the atomic percentage of carbon, oxygen, nitrogen, and sulfur was 72.80%, 21.40%, 4.14%, and 1.66%, respectively, which indicates the presence of ANSA grafted mainly onto the edges of GO or even on its surface. To our delight, EDS elemental mapping showed that the amount of N element was significantly lower than that of other elements, especially the S element. In fact, both strong SO_3H Brønsted acid centers and amidic NH basic centers exist simultaneously in the structure of GO-ANSA (**1**). This leads to a rapid proton transfer reaction from SO_3H to the amidic NH. This proton transfer has two significant consequences: it renders the free electron pair of nitrogen unavailable and alters its electronic levels. Ultimately, the number of allowed electron transfers involving N is reduced compared to other elements. Interestingly, this observation aligns with findings reported in the literature.[90]

FTIR spectra of GO, ANSA, and GO-ANSA (**1**) are shown in Fig. 3. In the FTIR spectrum of GO, the broad bands at 2400 cm^{-1} to 3600 cm^{-1} are related to the O–H group of carboxylic, alcoholic or phenolic functional groups.[91] The stretching vibrations at 1623 cm^{-1} and 1716 cm^{-1} are related to the C=C bonds in aromatic rings and the C=O bond in carboxylic acid, respectively.[92] The bonds at 1178 cm^{-1} and 1070 cm^{-1} show the vibrational stretching of the C–O bond in the phenol and alcohol groups, respectively.[93] In the FTIR spectrum of GO-ANSA (**1**), there was a broad peak at 3100 cm^{-1} to 3600 cm^{-1}, which shows the vibrational stretching of O–H in

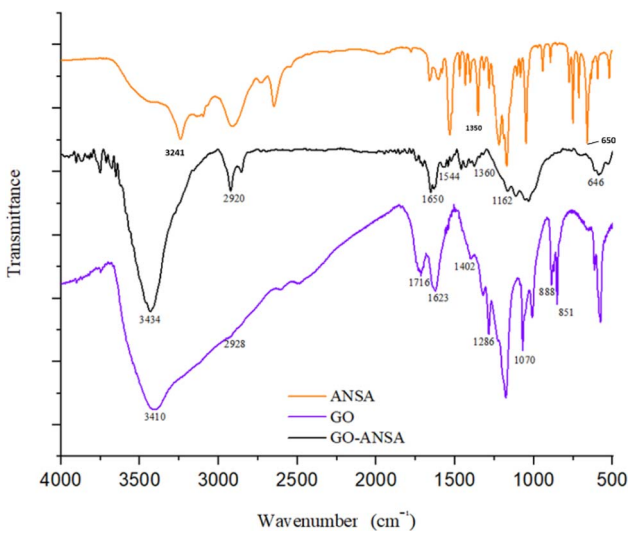

Fig. 3 FT-IR spectra of GO, ANSA, and GO-ANSA.

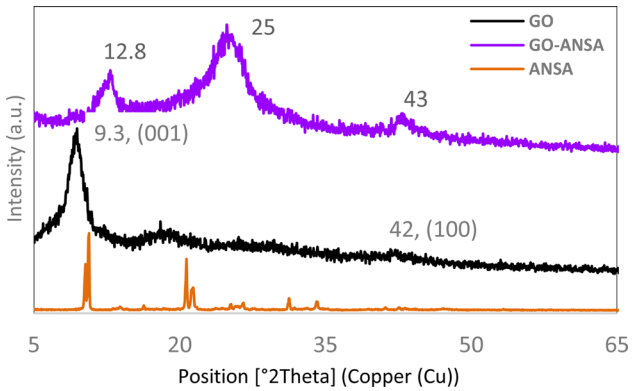

Fig. 4 XRD patterns of ANSA, GO and GO-ANSA (**1**) are shown from bottom to top.

sulfonic acid and hydroxyl groups as well as N–H in amide groups. Therefore, the carboxylic acid groups of GO were converted to the corresponding ones. The CH_2 asymmetric stretching vibration was observed at 2920 cm^{-1}.[91] The band that appeared at 1650 cm^{-1} showed the stretching vibration of the carbonyl groups in amide and confirmed the existence of amide functional group in the GO-ANSA. Also, the absorption band at 1544 cm^{-1} can be attributed to a combination of two absorptions related to the stretching vibration of C–N bond and the bending vibration of N–H bond in the secondary amide structures.[94]

The XRD pattern for GO showed a peak with a very high intensity at $2\theta = 9.3°$ (001) and another peak at about $2\theta = 42.0°$ (100), which confirmed the successful formation of GO.[95,96] After the functionalization of GO, the intensity of its corresponding peak was reduced in the XRD pattern of GO-ANSA (**1**). Both peaks were slightly shifted, which indicated the formation of a covalent bond between the functional groups of GO and ANSA. These observations are in agreement with the literature data on covalent-functionalization of GO by using different organic groups.[97–102] GO and GO-ANSA interlayer d spacing is 0.69 and 0.95 nm, respectively. Also, a new peak appeared at $2\theta = 25.0°$, which was due to the addition of ANSA compound to GO (Fig. 4).

Atomic force microscopy (AFM) was used to visualize the surface morphology of the sample and determine the maximum peak height—R_{max}, which is the highest peak above the mean line in the profile. The scanned area was 2 × 2 μm^2. The large-area GO's and GO-ANSA's AFM images and the corresponding deposited on a mica substrate are shown in Fig. 5. From the set of FE-SEM and AFM photographs taken, the most characteristic and repeatable images of the sample surface were selected for presentation. GO-ANSA's AFM images demonstrated that the morphology of GO changed after the catalyst preparation process and required calculations. The thickness of GO sheets was found to be 1.2 nm from the AFM images (Fig. 5e). However, the thickness increased to 2.1 nm in GO-ANSA, as shown in Fig. 5f.[103] FESEM images were used to determine the morphology of GO and GO-ANSA (**1**) (Fig. 5). The FESEM images of prepared GO showed the formation of its layered structure. The two-dimensional and layered structure of GO is

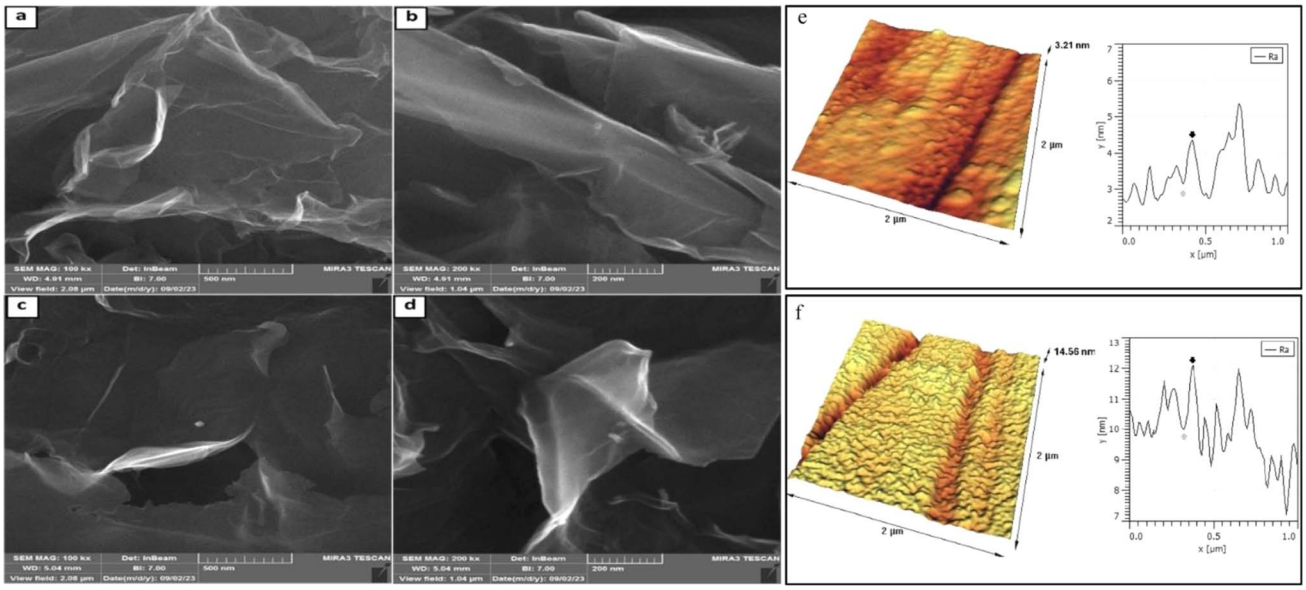

Fig. 5 FE-SEM images (a and b) for GO and (c and d) for GO-ANSA; atomic force microscopy measurement of (e) GO and (f) GO-ANSA (scanned area: 2 μm × 2 μm).

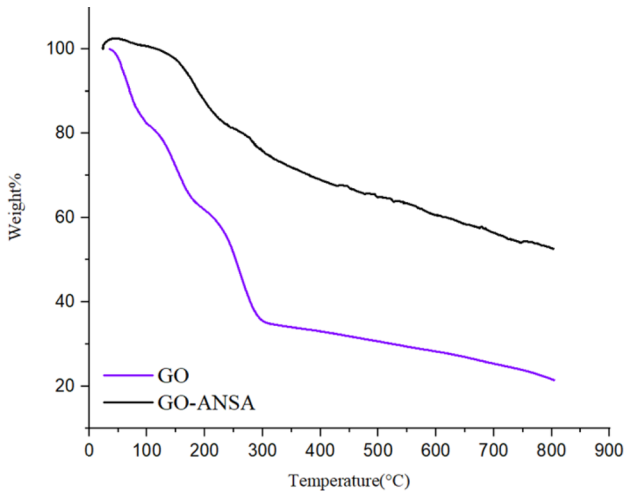

Fig. 6 The TGA analysis of GO and GO-ANSA (1).

a consequence of utilizing of the Hummers' method by starting from graphite with a three-dimensional structure (Fig. 5a and b). GO-ANSA's FESEM images showed the morphology of GO changed after the catalyst preparation process (Fig. 5c and d).

Thermogravimetric analysis (TGA) and differential thermogravimetric analysis (DTA) were carried out in the inert atmosphere of Ar at the range of 25–800 °C for both GO and GO-ANSA (**1**) (Fig. 6). The TGA diagram of GO showed three sharp decreases in the initial weight. The decrease of sample's weight before 100 °C and between 100–200 °C was related to the removal of absorbed water and pyrolysis of groups containing oxygen in GO (as CO and CO_2), respectively.[104] The third sharp drop occurred at 250–300 °C and can be attributed to the loss of carbon framework connections.[105] In the TGA of GO-ANSA, the increase in weight shown before 50 °C is due to the Buoyancy effects as well as absorption of water and CO_2. Also, the drop in weight at 150–200 °C is related to the removal of absorbed water. After that, the weight of the sample decreased with a gentle slope, which is due to the decomposition of functional groups in GO-ANSA and the desulfonation of SO_3H groups. After reaching 800 °C, GO lost more than 80% of its initial weight. Meanwhile, up to 50% of the weight of the GO-ANSA sample remained at the same thermal conditions. Therefore, the thermal stability of GO-ANSA is greatly increased by covalent bonding.

3.2. Catalytic activity assessment of the GO-ANSA nanomaterial (1)

To show the efficiency of GO-ANSA (**1**) and determine the optimized conditions, the three-component reaction of 4-chlorobenzaldehyde (**2a**, 1.0 mmol) and dimedone (**3b**, 2.0 mmol) for synthesis of the corresponding tetraketone (2,2′-((4-chlorophenyl)methylene)bis(3-hydroxy-5,5-dimethylcyclohex-2-en-1-one), **4a**) was studied as the model reaction. The results are summarized in Table 1. Therefore, various parameters including the type of solvent, amount of the catalyst loading, and temperature of the reaction were evaluated on the model reaction. Initially, the reaction was carried out without a catalyst and only a trace of the desired product **4a** was formed after 3 h (Table 1, entry 1). Then, GO was used in EtOH as a solvent, which resulted in a moderate isolated yield of 58% (entry 2). Furthermore, the reaction was carried out in the presence of GO-ANSA nanomaterial (**1**) in both water and EtOH under reflux conditions (entries 3 and 4) with higher efficiencies than the reaction in other solvents including THF, CH_2Cl_2, MeCN, MeOH and EtOAc (entries 6–10). In conclusion, EtOH as an effective and green solvent under reflux conditions is the best medium for the reaction. Therefore, all subsequent experiments to

Table 1 Optimization of the three-component reaction for the synthesis of **4a** catalyzed by the GO-ANSA[a]

Entry	Catalyst **1** loading (mg)	Solvent	Temp. (°C)	Time (min)	Yield[b] (%)
1	—	EtOH	100	180	Trace
2	10[c]	EtOH	Reflux	60	58
3	10	H_2O	Reflux	150	88
4	10	EtOH	Reflux	35	93
5	10	EtOH/H_2O (1 : 1)	Reflux	140	91
6	10	THF	Reflux	330	70
7	10	CH_2Cl_2	Reflux	360	42
8	10	MeCN	Reflux	270	82
9	10	MeOH	Reflux	180	85
10	10	EtOAc	Reflux	120	78
11	10	EtOH	R.T.	180	43
12	10	EtOH	50	120	55
13	5	EtOH	Reflux	45	89
14	15	EtOH	Reflux	20	97
15	20	EtOH	Reflux	20	96

[a] Reaction conditions: 4-chlorobenzaldehyde (**2**, 1.0 mmol) and dimedone (**3b**, 2.0 mmol) catalyzed by GO-ANSA (**1**). [b] Yields refer to the isolated products. [c] GO was used instead of GO-ANSA.

investigate the catalytic activity of GO-ANSA nanomaterial (**1**) were performed in EtOH. By increasing the amount of catalyst loadings in the model reaction, due to more concentration of acidic sites, the reaction efficiency reached the maximum efficiency (97%) in the minimum possible time (15 min). Indeed, increasing the catalyst loading to 15.0 mg resulted in higher production of the desired product **4a** in a shorter reaction time under the same conditions (entry 14). However, a further increase in the amount of loaded catalyst **1** did not significantly affect the yield and reaction time (entry 15).

Different derivatives of tetraketone **4a–p** were obtained under the optimized reaction conditions (4-amino-3-hydroxy-1-naphthalene sulfonic acid-functionalized GO (GO-ANSA) loading of 15.0 mg in EtOH under reflux conditions) using various aldehydes and enolizable compounds with very high efficiency (Table 2). The results showed that the desired products **4** were prepared in excellent yields and short reaction times. Furthermore, the presence of electron-withdrawing groups on the aromatic ring of aldehyde has a favourable effect on the reaction time compared to electron-donating groups. In addition, the presence of halogen atoms on the aromatic ring of the aldehyde acted as electron-withdrawing groups due to predominance of inductive effects on resonance ones. Therefore, the presence of the halogen atoms on the aromatic ring increases the yield and reduces the required reaction time. Furthermore, sensitive aldehydes having C=C bonds such as cinnamaldehyde survived very well under the

Table 2 Synthesis of tetraketone derivatives **4a–p** from different aldehydes **2** and enolizable compounds **3a–b** catalyzed by the GO-ANSA (**1**), as a heterogeneous nanocatalyst, under the optimized conditions[a]

Entry	R–CHO **2**	R_2	Time (min)	Product **4**	Yield[b] (%)	Mp (°C) found	Mp (°C) reported
1	4-Chlorobenzaldehyde	**3b**	20	**4a**	97	145–146	140–142 (ref. 107)
2	2-Chlorobenzaldehyde	**3b**	40	**4b**	90	204–206	205 (ref. 108)
3	4-Bromobenzaldehyde	**3b**	25	**4c**	94	157	158–159 (ref. 109)
4	4-Formylbenzonitrile	**3b**	20	**4d**	96	165–168	165–167 (ref. 109)
5	4-Hydroxybenzaldehyde	**3b**	40	**4e**	88	187–188	188–190 (ref. 109)
6	4-Methoxybenzaldehyde	**3b**	35	**4f**	88	141	142–143 (ref. 83)
7	2-Methoxybenzaldehyde	**3b**	45	**4g**	89	179–181	187–188 (ref. 108)
8	4-Nitrobenzaldehyde	**3b**	20	**4h**	96	188–190	188–190 (ref. 110)
9	3-Nitrobenzaldehyde	**3b**	30	**4i**	91	195–198	197–198 (ref. 71)
10	(*Z*)-3-Phenylacrylaldehyde (cinnamaldehyde)	**3b**	45	**4j**	86	215–217	215–217 (ref. 108)
11	4-Chlorobenzaldehyde	**3a**	20	**4k**	96	205	204–206 (ref. 111)
12	2-Chlorobenzaldehyde	**3a**	45	**4l**	87	230–232	229–231 (ref. 111)
13	4-Bromobenzaldehyde	**3a**	25	**4m**	92	239–242	240–241 (ref. 83)
14	4-Hydroxybenzaldehyde	**3a**	45	**4n**	88	192–195	192–194 (ref. 111)
15	4-Methoxybenzaldehyde	**3a**	35	**4o**	86	196	193–195 (ref. 111)
16	3-Nitrobenzaldehyde	**3a**	35	**4p**	90	207–211	209–210 (ref. 112)

[a] Condition of reaction: different aldehydes (**2**, 1.0 mmol) and enolizable compounds (**3a–b**, 2.0 mmol) catalyzed by the GO-ANSA (**1**) loading of 15.0 mg in EtOH under the reflux condition. [b] Yields refer to isolated products.

Table 3 Comparison of the catalytic efficiency of GO-ANSA with some previously reported heterogenous or homogeneous catalysts

Entry	Catalyst	Catalyst loading	Conditions	Time	Yield (%)
1	NaOH[113]	5 mg	H_2O/sonic./R.T.	60–90 min	65–84
2	$HClO_4$–SiO_2 (ref. 107)	50 mg	MeCN/reflux	6 h	54
3	TiO_2/SO_4^{2-} (ref. 114)	100 mg	Solvent free/R.T.	48 h	38–90
4	L-Histidine/ionic liquid[69]	30 mg	[bmim]BF_4/60 °C	40 min	60–75
5	Nano SiO_2Cl[70]	10 mg	$CHCl_3$/40 °C	1–4 h	70–90
6	Amino-appended β-cyclodextrin[71]	64 mg	H_2O/R.T.	1–5 h	58–96
7	Nano Cu–SiO_2 (ref. 115)	100 mg	EtOH/80 °C	30–75 min	90–97
8	$Cu_2(NH_2\text{-BDC})_2$(DABCO)[72]	40 mg	H_2O/reflux	30 min	98
9	Fe-zeolite[73]	30 mg	Toluene/160 °C	8 h	84
10	2-Aminopyrazine[74]	285 mg	ACN/80 °C	2 h	76–86
11	GO-ANSA	15 mg	EtOH/reflux	20–45 min	86–97

Table 4 Optimization of the three-component reaction for synthesis of **6b** catalyzed by the GO-ANSA[a]

Entry	Catalyst loading (mg)	Solvent	Temp. (°C)	Time (min)	Yield[b] (%)
1	10[c]	EtOH	Reflux	180	39
2	10	H_2O	Reflux	60	71
3	10	EtOH	Reflux	25	94
4	10	EtOH/H_2O (1 : 1)	Reflux	50	82
5	10	THF	Reflux	220	40
6	10	MeCN	Reflux	150	54
7	10	MeOH	Reflux	210	50
8	10	EtOAc	Reflux	240	38
9	10	EtOH	R.T.	260	44
10	10	EtOH	50	140	67
11	2.5	EtOH	Reflux	70	86
12	5	EtOH	Reflux	50	89
13	15	EtOH	Reflux	30	95

[a] Reaction conditions: 4-chlorobenzaldehyde (**2**, 1.0 mmol), dimedone (**3b**, 1.0 mmol) and malononitrile (**5**, 1.0 mmol) catalyzed by the GO-ANSA (**1**). [b] Yields refer to the isolated products. [c] GO was used instead of GO-ANSA.

optimized conditions and afforded corresponding tetraketone (**4j**) in high yield without polymerization.[106]

To demonstrate the superior catalytic activity of GO-ANSA (**1**) for the synthesis of tetraketone derivatives under the optimized conditions, the obtained results have been compared with the previous methods reported in the literature (Table 3).

Additionally, to evaluate the effectiveness of the optimized conditions and catalytic performance of GO-ANSA (**1**), another model reaction was chosen involving multi-component heteroannulation of 4-chlorobenzaldehyde (**2**), dimedone (**3b**) and malononitrile (**5**) in a 1 : 1 : 1 molar ratio for the synthesis of tetrahydrobenzo[*b*]pyrans. The results are summarized in Table

Table 5 Synthesis of tetrahydrobenzo[*b*]pyran derivatives **6a–k** from different aldehydes **2**, enolizable compounds **3a–b** and malononitrile (**5**) catalyzed by the GO-ANSA (**1**), as heterogeneous nanocatalyst, under optimized conditions[a]

Entry	R–CHO **2**	R_2	Product **6**	Time (min)	Yield[b] (%)	Mp (°C) found	Mp (°C) reported
1	Benzaldehyde	**3b**	**6a**	30	89	230–232	231–233 (ref. 76)
2	4-Chlorobenzaldehyde	**3b**	**6b**	25	94	210–212	209–211 (ref. 79)
3	4-Formylbenzonitrile	**3b**	**6c**	25	92	211	212–213 (ref. 76)
4	3-Nitrobenzaldehyde	**3b**	**6d**	15	96	214–216	214–216 (ref. 80)
5	4-Methoxybenzaldehyde	**3b**	**6e**	35	91	187–189	186–188 (ref. 76)
6	Benzaldehyde	**3a**	**6f**	45	85	267–239	239–241 (ref. 82)
7	4-Chlorobenzaldehyde	**3a**	**6g**	35	91	226–229	224–226 (ref. 77)
8	2-Chlorobenzaldehyde	**3a**	**6h**	20	92	210–213	212–214 (ref. 77)
9	4-Hydroxybenzaldehyde	**3a**	**6i**	35	82	235–339	234–236 (ref. 82)
10	4-Nitrobenzaldehyde	**3a**	**6j**	30	90	234–237	234–236 (ref. 60)
11	4-Methylbenzaldehyde	**3a**	**6k**	50	84	224.5	223–225 (ref. 82)

[a] Reaction conditions: different aldehydes (**2**, 1.0 mmol), enolizable compounds (**3a–b**, 1.0 mmol) and malononitrile (**5**, 1.0 mmol) catalyzed by the GO-ANSA (**1**) loading of 10.0 mg in EtOH under reflux conditions. [b] Yields refer to the isolated products.

4. Although the reaction can be performed in the presence of GO, as a catalyst rather than a support, it afforded a low yield and required a longer reaction time (entry 1). Interestingly, in the synthesis of tetrahydrobenzo[*b*]pyran derivatives, the best catalytic performance was observed in EtOH under reflux conditions similar to tetraketones (entries 2–8). The effect of temperature on the yield of model reaction was investigated (entries 9 and 10). The optimal quantity of catalyst **1** loading was also studied in the next experiments and the obtained data showed that the yield of the reaction was improved by increasing the amount of GO-ANSA (**1**) loading in the reaction mixture (entries 11–13). However, increasing the amount of loaded catalyst further than 10.0 mg did not significantly impact the yield of the reaction or have an adverse effect on the reaction time (entry 13).

Different tetrahydrobenzo[*b*]pyran derivatives **6a–k** were obtained under optimized reaction conditions (GO-ANSA loading of 10.0 mg in EtOH under reflux conditions) using various aldehydes, dimedone or 1,3-cyclohexanedione (**3a–b**), and malononitrile with very high efficiency (Table 5). After completion of the reaction, the nanocatalyst **1** was easily separated from the reaction mixture by filtration. All tetrahydrobenzo[*b*]pyran derivatives were prepared in high to excellent yields and very short times. The rate of reactions and efficiency were significantly affected by the nature of the functional groups on the aromatic ring of aldehydes. Consequently, the preparation of tetrahydrobenzo[*b*]pyrans by using aldehydes with electron-withdrawing groups requires shorter times than aldehydes with electron-donating groups.

3.3. Reusability of the catalyst

To test the reusability of GO-ANSA (**1**) as a heterogeneous nanocatalyst, it was separated from the reaction mixture (**4a** and **6b**) after completion of the reaction and washed with hot EtOH, then dried in an oven at 60 °C. The separated catalyst **1** was added to the model reaction. It was repeated five times under the same conditions and no significant change in the reaction yields was observed in both studied model reactions. The results in the synthesis of both tetraketone **4a** and tetrahydrobenzo[*b*]pyran **6a** derivatives are shown in Fig. 7. The recyclability of GO-ANSA catalyst (**1**) demonstrates that GO-ANSA could be used at least five times without meaningful loss in its catalytic performance.

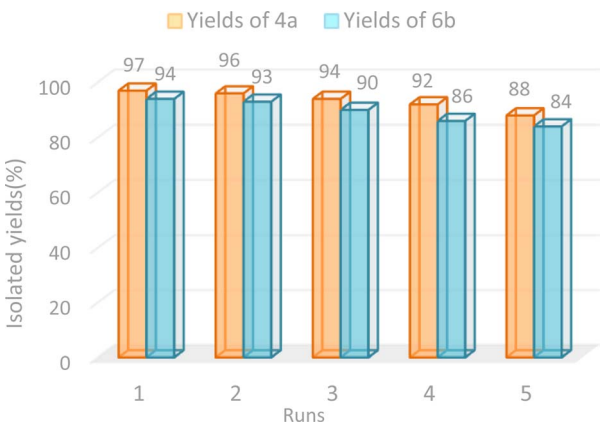

Fig. 7 Recycling results of GO-ANSA for the synthesis of **4a** and **6b**.

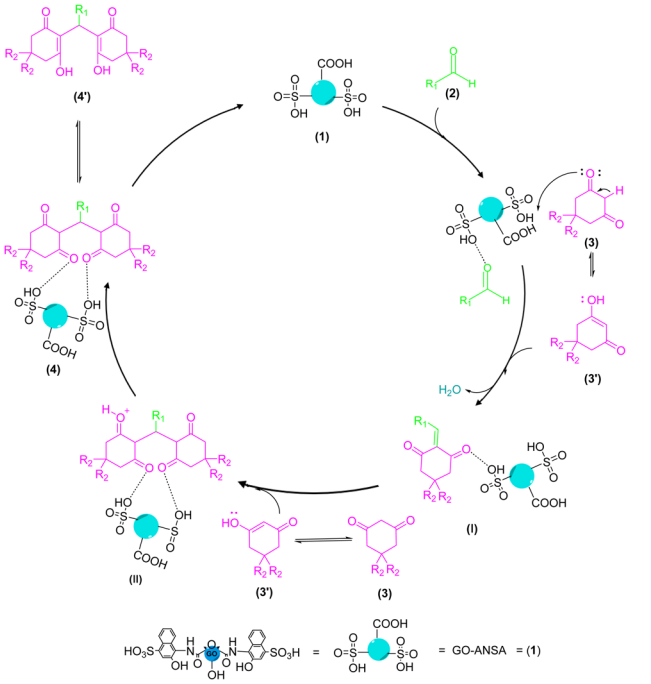

Scheme 3 A proposed mechanism for the synthesis of tetraketone derivatives **4** catalyzed by the GO-ANSA (**1**).

3.4. Proposed mechanism

The proposed mechanism for the GO-ANSA (**1**)-catalyzed reaction of aldehydes and two equivalent of enolizable compounds

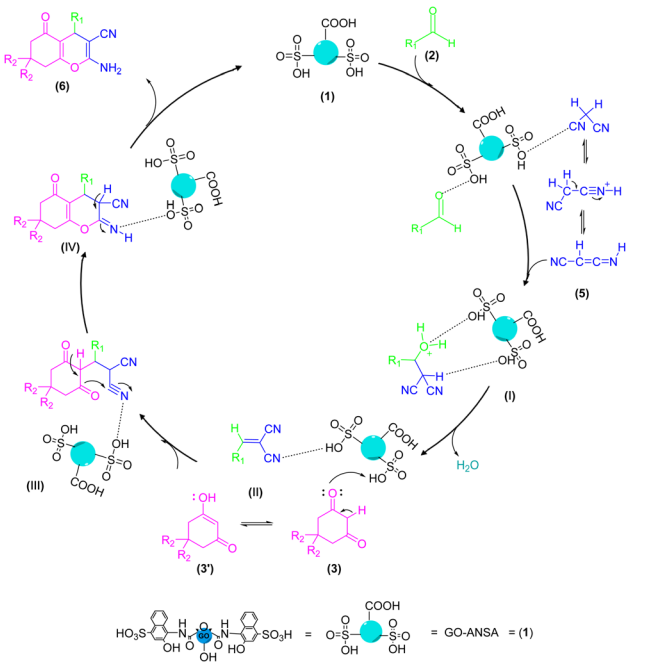

Scheme 4 A proposed mechanism for the synthesis of tetrahydrobenzo[*b*]pyran derivatives **6** catalyzed by the GO-ANSA (**1**).

is shown in Scheme 3. GO-ANSA contains SO_3H and carboxylic acid functional groups in its structure and leading to protonation of the carbonyl group of aldehydes **2**, thus increasing its nucleophilicity.[88] On the other hand, enolizable compounds are in equilibrium with their enolic form and the acidic catalyst accelerates this process. Then, by removing a water molecule, the Knoevenagel intermediate (**I**) is formed. Another equivalent of the enolizable compound **3**, after taking proton from the catalyst **1** and subsequent transformation into its enolic form), reacts with the intermediate **I** to form the intermediate **II** *via* Michael addition. After formation of the tetraketone compounds **4**, it can be in equilibration with its enol tautomer **4′** (Scheme 3).[83]

The proposed mechanism for the GO-ANSA (**1**)-catalyzed one-pot reaction of aldehydes **2**, enolizable compounds **3**, and malononitrile (**5**) is shown in Scheme 4. Protonation of all three compounds, *i.e.*, carbonyl groups of aldehydes, as well as enolizable compounds, and nitrile of malononitrile, occurred through the SO_3H groups present in the structure of the nanocatalyst **1**. This initial activation accelerates the Knoevenagel condensation of malononitrile (its imine–ketene resonance form) and aldehydes to afford intermediate **I**. Then, by removing a water molecule, intermediate **II** was formed through Knoevenagel condensation. The addition of the activated enolizable compound with this intermediate forms the intermediate **III** through Michael addition. Eventually, the final product **6** is obtained by through heteroannulation of the intermediate **III** and subsequent tautomerization of the intermediate **IV**.[78]

4. Conclusions

In this research, GO-ANSA was prepared as a new reusable carbocatalyst. The efficiency of this new nano-ordered catalyst was evaluated for the green synthesis of tetraketone as well as tetrahydrobenzo[*b*]pyran derivatives through one-pot MCRs in EtOH as a green solvent. The GO-ANSA catalyst showed high efficiency in both reactions and all of the derivatives were obtained in high to excellent yields and short reaction times. In this work, we used a novel heterogeneous nanocatalyst, which showed very beneficial activity compared to the previously reported methods in the literature. In addition, the catalyst was easily recovered and reused at least five times without a significant decrease in its activity. Among the advantages of the presented method, other features including high yield of the products without the formation of by-products, simple process, and mild and eco-friendly reaction conditions can be mentioned.

Author contributions

Sara Gharghish: writing – original draft, software, methodology, investigation, formal analysis, data curation. Mohammad G. Dekamin: writing – review & editing, visualization, validation, supervision, resources, project administration, funding acquisition, conceptualization. Sepideh Hasanzadeh Banakar: methodology.

Conflicts of interest

There are no conflicts to declare.

Acknowledgements

We are grateful for the partial financial support from The Research Council of Iran University of Science and Technology (IUST), Tehran, Iran (grant no 160/23372). We would also like to acknowledge the support of The Iran Nanotechnology Initiative Council (INIC), Iran.

Notes and references

1 R. Yang, Y. Wang, D. Wu, Y. Deng, Y. Luo, X. Cui, X. Wang, Z. Shu and C. Yang, *ACS Nano*, 2017, **11**, 7710–7718.
2 E. Alonso, F. R. Field and R. E. Kirchain, *Environ. Sci. Technol.*, 2012, **46**, 12986–12993.
3 A. H. C. Hart, R. Koizumi, J. Hamel, P. S. Owuor, Y. Ito, S. Ozden, S. Bhowmick, S. A. S. Amanulla, T. Tsafack, K. Keyshar, R. Mital, J. Hurst, R. Vajtai, C. S. Tiwary and P. M. Ajayan, *ACS Appl. Mater. Interfaces*, 2017, **9**, 13742–13750.
4 S. Hao, B. Ouyang, C. Li, B. Zhang, J. Feng, J. Wu, M. Srinivasan and Y. Huang, *J. Phys. Chem. C*, 2019, **123**, 8599–8606.
5 N. Zulfiqar, R. Nadeem and O. A. Musaimi, *ACS Omega*, 2024, **9**, 7986–8004.
6 R. K. Sharma, S. Gulati and S. Mehta, *J. Chem. Educ.*, 2012, **89**, 1316–1318.
7 R. P. Sourkouhi, M. G. Dekamin, E. Valiey and M. Dohendou, *Carbohydr. Polym. Technol. Appl.*, 2024, **7**, 100420.
8 S. J. Jeon, H. Li and P. J. Walsh, *J. Am. Chem. Soc.*, 2005, **127**, 16416–16425.
9 M. Toorbaf, L. Moradi and A. Dehghani, *J. Mol. Struct.*, 2023, **1294**, 136335.
10 M. G. Dekamin, M. Azimoshan and L. Ramezani, *Green Chem.*, 2013, **15**, 811–820.
11 J. W. J. Ang, *J. Chem. Educ.*, 2021, **98**, 203–207.
12 A. Mishra, P. Yadav and S. K. Awasthi, *ACS Org. Inorg. Au*, 2023, **3**, 254–265.
13 N. Nikooei, M. G. Dekamin and E. Valiey, *Res. Chem. Intermed.*, 2020, **46**, 3891–3909.
14 C. Wang, R. Ciganda, L. Yate, J. Tuninetti, V. Shalabaeva, L. Salmon, S. Moya, J. Ruiz and D. Astruc, *J. Mater. Chem. A*, 2017, **5**, 21947–21954.
15 M. S. Islam, S. M. Sarkar, M. L. Rahman, K. Hasan and E. J. O'Reilly, *Chem. Eng. J.*, 2024, **483**, 149271.
16 N. Ghanbari and H. Ghafuri, *Heliyon*, 2023, **9**, e20978.
17 B. Zheng, L. Chen, L. He, H. Wang, H. Li, H. Zhang and S. Yang, *Ind. Crops Prod.*, 2024, **210**, 118058.
18 H. M. A. Sharif, A. Mahmood, H. Y. Cheng, R. Djellabi, J. Ali, W. L. Jiang, S. S. Wang, M. R. Haider, N. Mahmood and A. J. Wang, *ACS Appl. Nano Mater.*, 2019, **2**, 5310–5319.
19 Z. Alirezvani, M. G. Dekamin, F. Davoodi and E. Valiey, *ChemistrySelect*, 2018, **3**, 10450–10463.

20 Y. H. Song, Q. T. Xu, T. He, Z. Y. Wang and L. Yu, *ACS Omega*, 2020, **5**, 21137–21144.
21 C. L. Weaver, J. M. Larosa, X. Luo and X. T. Cui, *ACS Nano*, 2014, **8**, 1834–1843.
22 Z. Zhang, M. Wang, D. Gao, D. Luo, Q. Liu, J. Yang and Y. Li, *Langmuir*, 2016, **32**, 10253–10258.
23 G. P. Kotchey, B. L. Allen, H. Vedala, N. Yanamala, A. A. Kapralov, Y. Y. Tyurina, J. Klein-Seetharaman, V. E. Kagan and A. Star, *ACS Nano*, 2011, **5**, 2098–2108.
24 Y. Zhou, K. Maleski, B. Anasori, J. O. Thostenson, Y. Pang, Y. Feng, K. Zeng, C. B. Parker, S. Zauscher, Y. Gogotsi, J. T. Glass and C. Cao, *ACS Nano*, 2020, **14**, 3576–3586.
25 M. Cobos, I. De-La-pinta, G. Quindós, M. D. Fernández and M. J. Fernández, *Nanomaterials*, 2020, **10**, 376.
26 W. Dai, Y. Liu, M. Wang, M. Lin, X. Lian, Y. Luo, J. Yang and W. Chen, *ACS Appl. Mater. Interfaces*, 2021, **13**, 19915–19926.
27 D. D. Kulkarni, I. Choi, S. S. Singamaneni and V. V. Tsukruk, *ACS Nano*, 2010, **4**, 4667–4676.
28 C. H. Rodríguez, J. d. J. P. Bueno, A. X. M. Pérez, M. R. Flores and G. Oza, *RSC Adv.*, 2023, **13**, 10621–10635.
29 S. Rana, G. B. B. Varadwaj and S. B. Jonnalagadda, *Nanoscale Adv.*, 2019, **1**, 1527–1530.
30 M. Eslami, M. G. Dekamin and E. Mahdavi, *Surf. Interfaces*, 2024, 104363.
31 D. Sah, J. Shabir, S. Surabhi, P. Gupta and S. Mozumdar, *Dalton Trans.*, 2021, **50**, 5644–5658.
32 Z. Zhang, X. Xiao, Y. Zhou, L. Huang, Y. Wang, Q. Rong, Z. Han, H. Qu, Z. Zhu, S. Xu, J. Tang and J. Chen, *ACS Nano*, 2021, **15**, 13178–13187.
33 D. Bradley, S. Sarpaki, V. Mirabello, S. G. Giuffrida, G. I. Kociok-Köhn, D. G. Calatayud and S. I. Pascu, *Nanoscale Adv.*, 2024, **6**, 2287–2305.
34 S. Caputo, A. Kovtun, F. Bruno, E. Ravera, C. Lambruschini, M. Melucci and L. Moni, *RSC Adv.*, 2022, **12**, 15834–15847.
35 K. Taheri, D. Elhamifar, S. Kargar and A. Zarnegaryan, *RSC Adv.*, 2023, **13**, 16067–16077.
36 J. Soni, N. Sahiba, A. Sethiya, P. Teli, D. K. Agarwal, A. Manhas, P. C. Jha, D. Joshi and S. Agarwal, *Polycyclic Aromat. Compd.*, 2022, **42**, 2970–2990.
37 Z. Ghadamyari, A. Khojastehnezhad, S. M. Seyedi and A. Shiri, *ChemistrySelect*, 2019, **4**, 10920–10927.
38 Z. Ghadamyari, A. Khojastehnezhad, S. M. Seyedi, F. Taghavi and A. Shiri, *ChemistrySelect*, 2020, **5**, 10233–10242.
39 A. Khojastehnezhad, M. Bakavoli, A. Javid, M. M. K. Siuki and M. Shahidzadeh, *Res. Chem. Intermed.*, 2019, **45**, 4473–4485.
40 Z. Ghadamyari, A. Shiri, A. Khojastehnezhad and S. M. Seyedi, *Appl. Organomet. Chem.*, 2019, **33**, 1–10.
41 S. Paul, S. Das, B. Mitra, G. C. Pariyar and P. Ghosh, *RSC Adv.*, 2023, **13**, 5457–5466.
42 M. G. Dekamin and M. Eslami, *Green Chem.*, 2014, **16**, 4914–4921.
43 S. D. Pasuparthy and B. Maiti, *ACS Omega*, 2022, **7**, 39147–39158.
44 S. Allameh, A. Davoodnia and A. Khojastehnezhad, *Chin. Chem. Lett.*, 2012, **23**, 17–20.
45 A. Yaghoubi, M. G. Dekamin and B. Karimi, *Catal. Lett.*, 2017, **147**, 2656–2663.
46 A. Malihishoja, M. G. Dekamin and M. Eslami, *RSC Adv.*, 2023, **13**, 16584–16601.
47 M. G. Dekamin, K. Varmira, M. Farahmand, S. Sagheb-Asl and Z. Karimi, *Catal. Commun.*, 2010, **12**, 226–230.
48 S. Kamalifar and H. Kiyani, *Polycyclic Aromat. Compd.*, 2022, **42**, 3675–3693.
49 H. Ostadzadeh and H. Kiyani, *Polycyclic Aromat. Compd.*, 2023, **43**, 9318–9337.
50 B. Borah, S. Swain, M. Patat, B. Kumar, K. K. Prajapat, R. Biswas, R. Vasantha and L. R. Chowhan, *Sci. Rep.*, 2023, **13**, 1–17.
51 P. Teli, A. Sethiya and S. Agarwal, *Res. Chem. Intermed.*, 2022, **48**, 731–750.
52 S. Singh, A. Kumar, L. Nebhani and C. K. Hazra, *JACS Au*, 2023, **3**, 3400–3411.
53 S. Siddiqui and Z. N. Siddiqui, *Nanoscale Adv.*, 2020, **2**, 4639–4651.
54 B. Maleki, M. Raei, E. Akbarzadeh, H. Ghasemnejad-Bosra, A. Sedrpoushan, S. S. Ashrafi and M. N. Dehdashti, *Org. Prep. Proced. Int.*, 2016, **48**, 62–71.
55 F. M. Moghaddam, S. Aghili, M. Daneshfar, H. Moghimi and Z. Daneshfar, *Res. Chem. Intermed.*, 2023, **49**, 1507–1543.
56 G. M. Maharvi, S. Ali, N. Riaz, N. Afza, A. Malik, M. Ashraf, L. Iqbal and M. Lateef, *J. Enzyme Inhib. Med. Chem.*, 2008, **23**, 62–69.
57 K. M. Khan, G. M. Maharvi, M. T. H. Khan, A. J. Shaikh, S. Perveen, S. Begum and M. I. Choudhary, *Bioorg. Med. Chem.*, 2006, **14**, 344–351.
58 J. M. Khurana and K. Vij, *J. Chem. Sci.*, 2012, **124**, 907–912.
59 T. Josephrajan and V. T. Ramakrishnan, *Can. J. Chem.*, 2007, **85**, 572–575.
60 A. R. Shendabadi, H. Tebyanian, R. Zare, M. G. Dekamin, H. Kooshki and J. Rashidiani, *Biointerface Res. Appl. Chem.*, 2020, **10**, 6706–6717.
61 Z. Akhlaghi, M. R. Naimi-Jamal, L. Panahi, M. G. Dekamin and B. F. Far, *Heliyon*, 2023, **9**, e13522.
62 M. A. Zolfigol, A. Khazaei, A. R. Moosavi-Zare, J. Afsar, V. Khakyzadeh and O. Khaledian, *J. Chin. Chem. Soc.*, 2015, **62**, 398–403.
63 K. K. Gangu, S. Maddila, S. B. Mukkamala and S. B. Jonnalagadda, *Ind. Eng. Chem. Res.*, 2017, **56**, 2917–2924.
64 F. Kalantari, H. Esmailipour, H. Ahankar, A. Ramazani, H. Aghahosseini, O. Kaszubowski and K. Ślepokura, *ACS Omega*, 2023, **8**, 25780–25798.
65 I. A. Azath, P. Puthiaraj and K. Pitchumani, *ACS Sustain. Chem. Eng.*, 2013, **1**, 174–179.
66 S. Agarwal, A. Sethiya, J. Soni, N. Sahiba and P. Teli, *Appl. Organomet. Chem.*, 2022, **36**, e6604.
67 P. Teli, N. Sahiba, A. Sethiya, J. Soni and S. Agarwal, *J. Heterocycl. Chem.*, 2021, **58**, 1393–1407.

68 M. Zabihzadeh, F. Shirini, H. Tajik and N. Daneshvar, *Polycyclic Aromat. Compd.*, 2021, **41**, 1972–1987.
69 Z. Yan and S. Zhicai, *Chin. J. Chem.*, 2010, **28**, 1184–1188.
70 R. Karimian, F. Piri, B. Karimi and A. Moghimic, *Croat. Chem. Acta*, 2011, **84**, 111–115.
71 Y. Ren, B. Yang and X. Liao, *RSC Adv.*, 2016, **6**, 22034–22042.
72 A. Džambić, S. Muratović, E. Veljović, A. Softić, E. Dautović, M. Š. Husejnović, E. Horozić and A. Smajlović, *Eur. Chem. Bull.*, 2020, **9**, 285–290.
73 S. Mondal, A. M. Pandey and B. Gnanaprakasam, *React. Chem. Eng.*, 2022, **8**, 855–862.
74 D. Thakur, M. Kaur, D. S. Malhi, S. Garg, A. Sharma and H. S. Sohal, *Monatsh. Chem.*, 2021, **152**, 537–543.
75 M. G. Dekamin, S. Z. Peyman, Z. Karimi, S. Javanshir, M. R. Naimi-Jamal and M. Barikani, *Int. J. Biol. Macromol.*, 2016, **87**, 172–179.
76 A. Khazaee, R. Jahanshahi, S. Sobhani, J. Skibsted and J. M. Sansano, *Green Chem.*, 2020, **22**, 4604–4616.
77 H. Alinezhad, M. Tarahomi, B. Maleki and A. Amiri, *Appl. Organomet. Chem.*, 2019, **33**, 1–14.
78 N. Rostami, M. G. Dekamin, E. Valiey and H. Fanimoghadam, *Sci. Rep.*, 2022, **12**, 1–12.
79 B. Maleki and S. S. Ashrafi, *RSC Adv.*, 2014, **4**, 42873–42891.
80 M. Kazemzad, A. A. Yuzbashi, S. Balalaie and M. Bararjanian, *Synth. React. Inorg., Met.-Org., Nano-Met. Chem.*, 2011, **41**, 1182–1187.
81 A. Yaghoubi and M. G. Dekamin, *ChemistrySelect*, 2017, **2**, 9236–9243.
82 M. A. Nasseri and S. M. Sadeghzadeh, *J. Iran. Chem. Soc.*, 2013, **10**, 1047–1056.
83 S. H. Banakar, M. G. Dekamin and A. Yaghoubi, *New J. Chem.*, 2018, **42**, 14246–14262.
84 M. G. Dekamin, F. Mehdipoor and A. Yaghoubi, *New J. Chem.*, 2017, **41**, 6893–6901.
85 M. Ishani, M. G. Dekamin and Z. Alirezvani, *J. Colloid Interface Sci.*, 2018, **521**, 232–241.
86 F. Davoodi, M. G. Dekamin and Z. Alirezvani, *Appl. Organomet. Chem.*, 2019, **33**, e4735.
87 A. Alinasab Amiri, S. Javanshir, Z. Dolatkhah and M. G. Dekamin, *New J. Chem.*, 2015, **39**, 9665–9671.
88 M. G. Dekamin and Z. Mokhtari, *Tetrahedron*, 2012, **68**, 922–930.
89 D. R. Joya-Cárdenas, J. P. Rodríguez-Caicedo, A. Gallegos-Muñoz, G. A. Zanor, M. S. Caycedo-García, C. E. Damian-Ascencio and A. Saldaña-Robles, *Nanomaterials*, 2022, **12**, 1–18.
90 S. S. Mortazavi, A. Abbasi and M. Masteri-Farahani, *Appl. Organomet. Chem.*, 2020, **34**, 1–12.
91 G. Surekha, K. V. Krishnaiah, N. Ravi and R. P. Suvarna, *J. Phys.: Conf. Ser.*, 2020, **1495**, 12.
92 A. A. Olorunkosebi, M. A. Eleruja, A. V. Adedeji, B. Olofinjana, O. Fasakin, E. Omotoso, K. O. Oyedotun, E. O. B. Ajayi and N. Manyala, *Diamond Relat. Mater.*, 2021, **117**, 108456.
93 G. Santamaria, E. G. B. Arojas, E. Q. Gonzalez, E. S. Mora, M. Q. Ruiz and J. D. S. Juarez, *Mater. Res. Express*, 2019, **6**, 31.
94 Y. Ji, X. Yang, Z. Ji, L. Zhu, N. Ma, D. Chen, X. Jia, J. Tang and Y. Cao, *ACS Omega*, 2020, **5**, 8572–8578.
95 A. Amoozadeh, S. Rahmani, M. Bitaraf, F. B. Abadi and E. Tabrizian, *New J. Chem.*, 2016, **40**, 770–780.
96 I. Sengupta, S. S. S. S. Kumar, S. K. Pal and S. Chakraborty, *J. Mater. Res.*, 2020, **35**, 1197–1204.
97 L. Irannejad, S. J. Ahmadi, S. Sadjadi and M. Shamsipur, *J. Iran. Chem. Soc.*, 2018, **15**, 111–119.
98 P. Li, S. Sun, A. Dong, Y. Hao, S. Shi, Z. Sun, G. Gao and Y. Chen, *Appl. Surf. Sci.*, 2015, **355**, 446–452.
99 M. Mirza-Aghayan, M. Mohammadi and R. Boukherroub, *J. Organomet. Chem.*, 2022, **957**, 122160.
100 T. Kuanyshbekov, Z. Sagdollin, E. Zhasasynov, K. Akatan and B. Kurbanova, *J. Compos. Sci.*, 2023, 1–16.
101 Y. Esmaeili, E. Bidram, A. Zarrabi, A. Amini and C. Cheng, *Sci. Rep.*, 2020, 1–13.
102 M. D. Pravin, C. F. S and A. Gnanamani, *RSC Adv.*, 2018, 38416–38424.
103 N. Huang, H. Lim, C. Chia, M. Yarmo and M. Muhamad, *Int. J. Nanomed.*, 2011, 3443–3448.
104 T. Wu, X. Wang, H. Qiu, J. Gao, W. Wang and Y. Liu, *J. Mater. Chem.*, 2012, **22**, 4772–4779.
105 Y. Feng, N. Feng, Y. Wei and G. Zhang, *RSC Adv.*, 2014, **4**, 7933–7943.
106 M. G. Dekamin, J. Mokhtari and M. R. Naimi-Jamal, *Catal. Commun.*, 2009, **10**, 582–585.
107 S. Kantevari, R. Bantu and L. Nagarapu, *J. Mol. Catal. A: Chem.*, 2007, **269**, 53–57.
108 E. C. Horning and M. G. Horning, *J. Org. Chem.*, 1946, 95–99.
109 F. Darviche, S. Balalaie, F. Chadegani and P. Salehi, *Synth. Commun.*, 2007, **37**, 1059–1066.
110 N. P. Chandia, J. C. Canales, I. Azocar, V. G. Pawar, W. M. D. Borggraeve and W. Dehaen, *Synth. Commun.*, 2000, 927–939.
111 J. K. Rajput and G. Kaur, *Catal. Sci. Technol.*, 2014, **4**, 142–151.
112 F. E. King and D. G. I. Felton, *J. Chem. Soc.*, 1946, 1371–1372.
113 G. Cravotto, A. Demetri, G. M. Nano, G. Palmisano, A. Penoni and S. Tagliapietra, *Eur. J. Org. Chem.*, 2003, 4438–4444.
114 T. S. Jin, J. S. Zhang and A. Q. Wang, *Synth. Commun.*, 2005, 2339–2345.
115 M. Gupta and M. Gupta, *J. Chem. Sci.*, 2016, **128**, 849–854.